Designing and Manufacturing University of South Carolina's First CubeSat Prototype

Shruti S. Jadhav[1] and Patrick A. Bailey[2]
University of South Carolina, Columbia, SC, 29201, USA

CubeSats have become increasingly popular for their cost-effectiveness and versatility in space exploration. Against this backdrop, the University of South Carolina has developed its first CubeSat prototype as part of a senior design project. This paper provides a detailed description of the planning, design, manufacturing, testing and evaluation phases of developing the CubeSat. This project aimed to demonstrate design competence by developing a CubeSat and ground station that has photo and data collection, storage, and transfer capabilities with a budget of $4,321, within 13 weeks. Under this generic framework, specific requirements such as surviving launch to Low Earth Orbit, taking a picture every minute on-board the CubeSat, storing pictures and other system information, receiving commands, and transmitting data from and to ground station respectively, and extending these functionalities during blackout, are some of the evaluation parameters for this work. In this process, preliminary conceptual designs were put forth and evaluated based on criteria devised by the team. This included conducting trade-offs to identify fitting concepts, drawing risk maps to determine potential hazards, and devising approaches to mitigate the hazards. With a selection of an initial design concept, the detailed design process included theoretical calculations along with a deeper exploration of each of the components of the CubeSat while considering the financial, weight and power budgets. Then, the manufacturing of CubeSat based on the detailed design was broken down into the creation of structure, provision of control and integration with code. To elaborate, the CubeSat features an aluminum structure that houses the components, with the Raspberry Pi Zero 2W acting as the computer on board. This is connected to a Pi camera module, long range (LoRa) radio transceiver, an inertial measurement unit (IMU), and a power management circuit. This power management circuit is connected to solar panels and a battery, providing, and distributing power to the system. Additionally, the data from the IMU is utilized to control the CubeSat's orientation with the help of flywheels connected to motors. The setup of the ground station includes a LoRa packet radio transceiver connected to a laptop. Lastly, the CubeSat is tested by demonstrating compliance with the requirements listed for the project. Furthermore, the design and work are evaluated in terms of compliance and use of standards, the social and environmental impact, and further improvements.

I. Nomenclature

g	=	Gravitational acceleration, m/s^2	A	=	Area, m^2
a	=	Acceleration, m/s^2	m	=	Mass, kg
C_d	=	Coefficient of Drag	r	=	Reflection factor
ρ	=	Density, kg/m^3	I	=	Moment of Inertia, kg*m^2
V	=	Velocity, m/s			

[1] Graduate Student, USC Student Media Manager, Department of Mechanical Engineering, AIAA Student Member.
[2] Graduate Student, USC Student Branch President, Department of Mechanical Engineering, AIAA Student Member.

II. Introduction

As humanity moves towards heavy space exploration, the past decades have seen a great enthusiasm for the outlook for space travel along with the push towards many unmanned missions to explore planets and asteroids. As such, the increase in space exploration using small satellites cannot go unnoticed. With a compound annual growth rate predicted of 16% from 2022 to 2032 for the small satellite market, the diverse applications in navigation, communication, earth observation, etc., make it an attractive choice for research and investment.[1] Within the area of small satellite space explorations, Nanosatellites, Microsatellites, Minisatellites, CubeSats, and many other variations can be used for desired mission applications. CubeSats are small satellites with basic unit form of 10 cm edge cube, namely 1U, which can be put together to form bigger artifacts.[2] A compact form, standard dimensions, and modular design makes CubeSats ideal platforms for an experience in systems engineering, spacecraft design, manufacturing, and operation.

Being the first CubeSat prototype for the University of South Carolina, this report discusses the senior design project for the CubeSat design and presents a thorough description of the project planning, design, manufacturing, and testing and evaluation of the CubeSat. The engineering design process in detail includes understanding the requirements, creating preliminary conceptual designs, followed by detailed design exploration, manufacturing of the CubeSat, testing for compliance and lastly evaluation with respect to use of standards. This process is elaborated in sections II through VII of this paper.

A. Problem Statement

With the goal of the project to "Design and build a CubeSat and appropriate ground station capable of receiving commands and transmitting sensor and system data," certain subtasks were drawn as part of the project planning to create well-defined project objectives. These include performing a structural analysis of primary loadbearing elements, take a photo every minute, store, analyze, interpret, and transmit data, survive static launch loads, survive blackout zones without solar power/communications, fit and fly inside of an unmanned aerial vehicle (UAV) designed by colleagues, and also comply with all legal requirements. Due to budget and time constraints, certain clarifications were added to the problem statement that exclude the launch and survival of the CubeSat in space, with design and testing for use on Earth. As a result, the designed mission of the CubeSat can be seen below in Fig. 1. Overall, the design competence is evaluated based on the development of a CubeSat and a ground station that can collect and transmit data on a budget of $4,321 in team of 4 under 13 weeks, with the CubeSat surviving launch to low earth orbit (LEO) and taking a photo every minute while storing and streaming data and receiving commands.

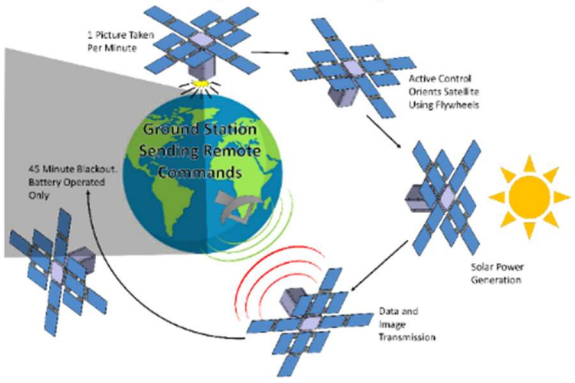

Fig. 1: Designed mission of CubeSat.

III. Conceptual Design

A comprehensive requirement analysis was conducted to understand exactly what functionalities must be accomplished by each subsystem for CubeSat to meet the given requirements within the given period. These included listing out mission functionalities such as power generation, attitude determination, capturing pictures among other related requirements, and understanding the specific data flow between different subsystems. Using the completed requirement analysis, multiple unique conceptual designs were put forth that were evaluated against each other using trade-offs, with the narrowed selection of concepts receiving further analysis through drawing risk maps and offering risk mitigation approaches. Some of these conceptual designs sketches are provided in Table 1 which include a brief description on their parts and operation, with an assumption for same ground station design with data receiving and processing unit for all design variations.

Table 1: Conceptual Design Sketches

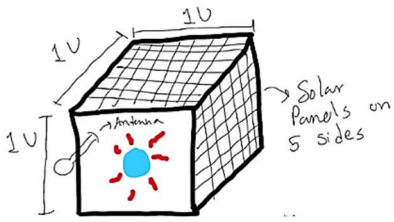	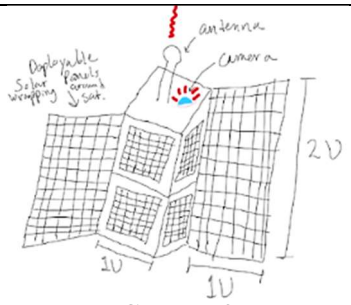	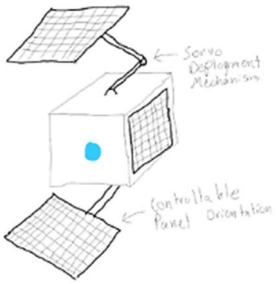
Concept 1 Size: IU Features: 1 omnidirectional antenna, 1 camera (blue dot), no controllability Solar panel: 5 sides	**Concept 2** Size: 2U Features: 1 Unidirectional antenna, 1 camera (blue dot), no controllability Solar panels: main body, 2 deployable (2U)	**Concept 3** Size: 1U Features: 1 omnidirectional antenna, 1 camera, controllable Solar panels: 3 main body, 2 deployable (1U), controlled deployment

A. Risk Evaluation and Design Options

A trade-off study was conducted between the conceptual designs. This study focused on the categories relating to the CubeSat such as development cost, manufacturability, reliability, time to completion, system weight, power generation and consumption, as well as volume limits. This tradeoff provided a deeper view into how feasible each design would be in all aspects such as making, integrating, and interaction of systems, not only within the CubeSat but also regarding constraints placed on weight and size requirements to be carried on an UAV, all within provided time frame. Risk maps were further developed for each of the design concepts to assess the risks that could affect the mission. Sample of the risk map for the 3rd design in Table 1, is provided in Fig 2a with the sample of some of the considered risks as following:

1. The CubeSat fails to get adequate power, either due to overconsumption or underproduction.
2. The CubeSat loses the use of its orientation control mechanism.
3. Deployable parts such as solar panels or antennas fail to deploy.
4. The CubeSat unintentionally loses communication with ground for reasons other than control system failure.
5. Code related failures.
6. The cameras are damaged by sun exposure.
7. Breakage due to launch and the forces involved.
8. Spin imparted on CubeSat and cameras unable to get clear photo.

The chart is created by placing risk according to the probability of the risk happening on the x-axis and the severity of the risk in affecting the mission on the y-axis. Additional risks such as collision in orbit, solar flares, among others were also considered in depth for all designs.

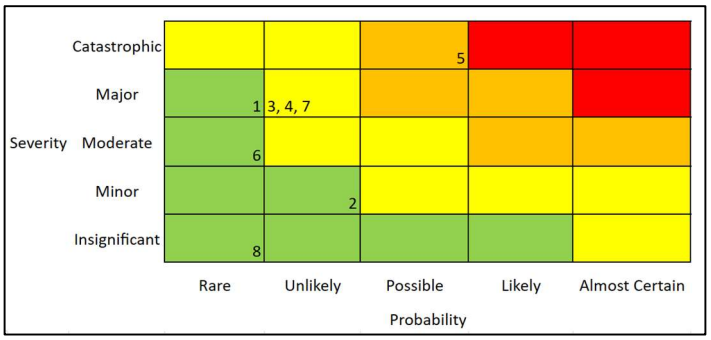

a)

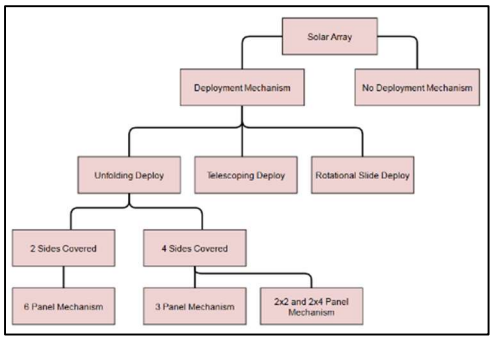

b)

Fig 2: Risk map for concept 3 (a) and DOT for solar array (b).

While no risks for any designs fell in the red zone, some risk mitigation approaches were derived to increase the reliability of the CubeSat. For the risk of code failure presented, it was decided to be mitigated with use of heavy code

testing with the desired use case, prior to finalizing the integration. Additionally, it was decided to incorporate redundancy and alternative approaches in the systems as a way of decreasing the risk of complete failure of a system. This applies in many ways such as having 2 cameras on board instead of one, having multiple solar panel deployment in case of single panel deployment failure, and continuous function of CubeSat independent of communications. Furthermore, measures such as structural analysis, with the magnitude and duration of the expected forces, can be taken to prevent the underlying risk of structural failure.

Due to the small degree of differences in the designs presented, many of them will use the same parts, or encounter similar problems. As a result, to facilitate the modularity of these narrowed ideas, Design Option Trees (DOT) are constructed that show the breakdown of concepts that can be implemented. These assist in the decision making for the design paths for the parts of the CubeSat. A sample of such DOT for the solar array is shown in Fig 2b.

IV. Detailed Design

The detailed design of the CubeSat focused on structural design and material choice, the equipment locations within the CubeSat for functionality, finite element analysis (FEA) simulations, on-orbit concerns, as well as the solar array design and deployment.

A. CubeSat Structural Design

Early investigations into the CubeSats internal structure led to the realization that many CubeSats followed one of 3 structural templates: using rigid framing only to connect to the outer shell, using a combination of thin wall structures and rigid framing, and using only a continuous layer of thin walls to surround and mount the internal components. As weight is a major concern for any satellite, and specifically this design because of the multi-mission purpose it had to serve for the senior design course, the hybrid approach of framing and thin walls was used in the structural design. A material tradeoff was in which the team selected Aluminum because of its strength-to-weight and proven applicability to space missions for both framing and the 0.5 mm thin walls.

The primary driver for this project was the overall form-factor and weight budget of 1.5 kg which determined the selection of electronics. Modifying the initial concept selected, a 1.5U CubeSat (10 cm x 10 cm x 17 cm) was designed for ease of internal component configuration and manufacturing. The measurements were determined from the outside-in because of the solar arrays thickness. Fig 3 provides a view of the internal wall structure of the CubeSat combining framing and thin walls (with some components visible), as well as a view of the CubeSat solar array deployed with its outer walls attached.

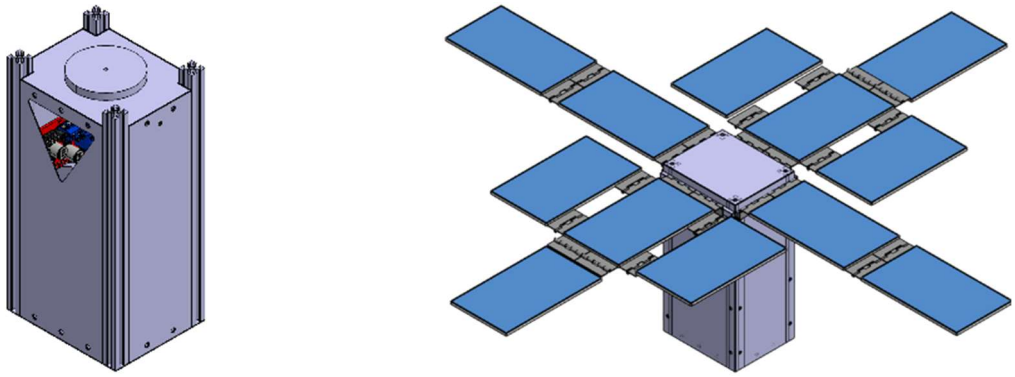

a) b)

Fig 3: Internal CubeSat structure (a), CubeSat with external structure and solar array (b).

The aluminum framing extends above the side walls to allow for better control. To achieve multi-axial rotation control, space was required for the flywheels used in momentum generation. Moreover, having the flywheels close together internally would pose manufacturing challenges, requiring relocation of one to external side with its motor mounted on the internal structure's ceiling. The side cutout in thin wall in Fig 3a was made for auxiliary powering during testing, and part installation once all walls were connected.

The internal component configuration contained a Pi Zero 2W, a LiPo battery for powering the system and storing energy from the solar panels, 2 motors, 1 motor controller, a battery controller, Inertial Measurement Unit (IMU), Radio, and 2 cameras for redundancy in operation. The positioning of these components required trial and error with consideration for the most centralized center of gravity (CG) to the origin of the system, as well as the length and complexity of wire routing. Internal views of the CubeSat components can be seen in Fig. 4.

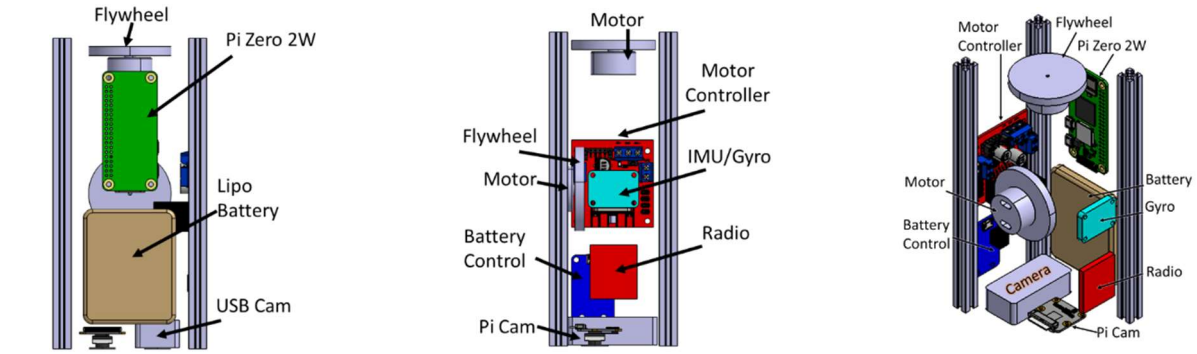

a) b) c)

Fig. 4: Wide side view (a), Short side view (b), Isometric view (c) of CubeSat internal structure.

Simplified FEA simulations were run on the CubeSat to validate the structural design. It is expected that the CubeSat will undergo significant vibrations during launch, radiation from the sun, as well as thermal cycling in space. However, due to time constraints, only *g*-loading was assessed as a preliminary measure of the design. The applied *g*-force was 15 *g*'s on the CubeSat had a safety factor of 1.5 applied to the simulation for a total of 22 *g*'s. The Von Mises stresses showed compression of only the CubeSat ceiling, with the lower surface not deforming due to the application of boundary conditions of a fixed/non-rotational lower surface. In its most critical area (the ceiling motor mount hole), the CubeSat experienced approximately 1 KPa being applied, leading to the max deformation of 7.2 µm. This shows that the structure does not have cause for concern of significant deformation, but additional safety factors can be employed internally through the addition of aluminum framing to support the ceiling-mounted motor. The structural FEA simulations are seen in Fig. 5.

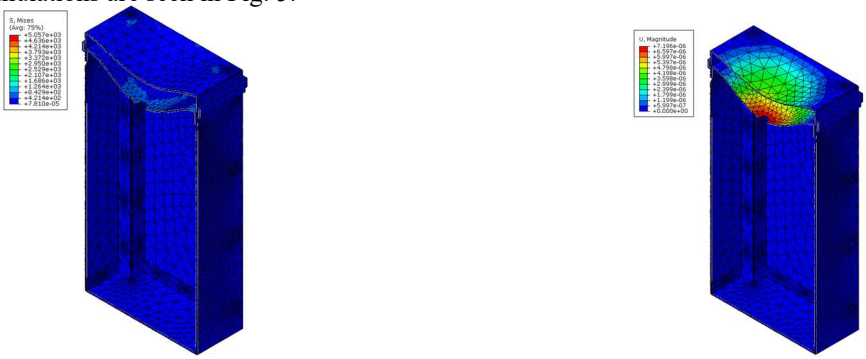

a) b)

Fig. 5: *g*-loading Von Mises stress (a), and internal wall displacement (b).

B. Operational Concerns and Calculations

The CubeSat was designed to operate in LEO, primarily because of its function to take pictures of earth, with needing to have a 90-minute revolution for power consumption with a 45-minute blackout. This means the satellite sits on a circular orbit at an altitude of 274.5 km and with a velocity of 7740 m/s. As a result of the orbit, aerodynamic drag cannot be ignored as it will slow down the CubeSat over time. Dividing the aerodynamic drag equation by the mass gives us the deceleration of the CubeSat due to drag using Eq. (1) below.

$$a_d = -\frac{1}{2}\rho\frac{C_d A}{m}V^2 \tag{1}$$

With a maximum cross-sectional area of 0.109 m^2 when the solar panels are fully deployed, and orbital velocity of 7740 m/s, an air density of 4.13 $x10^{-11}$ kg/m^3 at an altitude of 274.5 km, a mass of CubeSat approximated to be 1.29 kg, and the C_d approximated[3] to 2.2, the acceleration on the CubeSat due to drag is found to be approximately -2.3 $x10^{-4}$ m/s^2.

An estimation is required to determine how the CubeSat's orbit will be affected by solar radiation. Because the orbit altitude is less than 800 km, these effects will be less than aerodynamic drag.[3] With mass of 1.3 kg, a reflection factor of 0.02 for the solar panels, and 0.4 for the aluminum structure, yields an area weighted average reflection factor of 0.04. The acceleration on the CubeSat due to solar radiation is found to be -3.99 $x10^{-7}$ m/s^2 using Eq. (2) below.

$$a_s = -4.5 \cdot 10^{-6}\frac{A(1+r)}{m} \tag{2}$$

The CubeSat's life must be verified to make sure it can survive at least 1 full revolution. The calculation only considers the acceleration due to drag as solar radiation is assumed negligeable, with the Kármán line at 100 km altitude established as the reentry boundary. Multiplying the acceleration due to drag by the revolution time of 90-minutes divided by pi, gives a function of the rate of change of orbital altitude.[4] Upon integration of this function between the starting and finished altitude, a time to reenter is found to be approximately 5 days.

Lastly, the gravitational torques acting on the CubeSat need to be determined for the implementation of the active control system. Using the values for moments of inertia of the CubeSat in Z and Y, the maximum gravitational torque on the CubeSat was calculated as 8.67 x 10^{-5} N*m. This is an extremely small torque which can easily be counteracted by the satellite's attitude control system.

C. Solar Array and Power Generation

To generate enough power for continuous functional operation of the CubeSat, a solar array deployment mechanism is required to allow for an increased number of solar panels to face the sun. The deployment mechanism aims to deploy 12 solar panels to face the top side of the CubeSat. The deployment mechanism was determined to be a spring-loaded unfolding hinge, with the panel configuration of 2 folding panels on the short sides of the CubeSat, and a 4-panel folding configuration on the long sides. This also helps to maintain the CG of the CubeSat. The low carbon steel hinges are constrained to the solar panels using an aluminum harness on the back.

The hinges, being a moving component, would be a primary failure point in the system. Therefore, they required FEA simulation under the same launch loads as the CubeSat to determine its internal stresses and deformation. A safety factor of 1.5 was applied to the *g*-loading for a total of 22.5 *g*'s. Each solar panel weighs 31.6 grams, and the hinge mass is 4.1 grams, resulting in the 4-panel array's total mass of 151 grams. Under the *g*-loads, the 4-panel hinge experiences a load of 33.3 N. Fig 6 shows a max stress of 21.95 MPa is much less than that of the yield strength of 330 MPa. The displacement of these hinges is in µm. Additionally, Fig 7 shows deployment process of the solar panels, highlighting its compact form-factor in design.

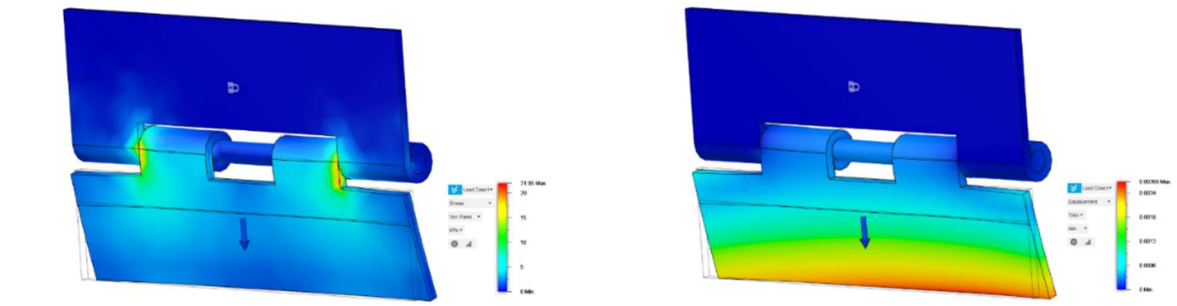

a) b)

Fig 6: Von Mises Stress (a), and displacement (b).

a) b) c)

Fig 7: Folded (a), deploying (b), and deployed (c) 4x solar array.

1.2 Watt panels that fit along the length of the CubeSat, with rated peak voltage of 6.07 V and peak current of 200 mA, were chosen for this design. All internal systems require 5 V to run, so the panels are wired in parallel to maximize the current, allowing for a max current supply of 2.4 A at 6 V for a total power supply of 14.4 W. Due to the blackout orbit of the CubeSat, an additional battery is needed to store energy, with half of the 14.4 W dedicated to recharging the on-board battery. A 1-cell 2500 mAh LiPo was selected for its superior energy density in this case. A battery management circuit was integrated for the simultaneous application of battery charging and power distribution by the solar panels. Since LiPo's should not be charged more than 0.5 times that of their mAh rating for safety purposes, the max stored current is 1250 mA, which is beneficial since half of the available current is right at 1200 mA. At 1200

mA for ¾ of an hour, the battery will only charge up to a bit over 36% of its max charge, allowing for 3.33 Wh of power usage. A complete wiring diagram depicting the supply of power and other relevant data connections is provided in Fig 8.

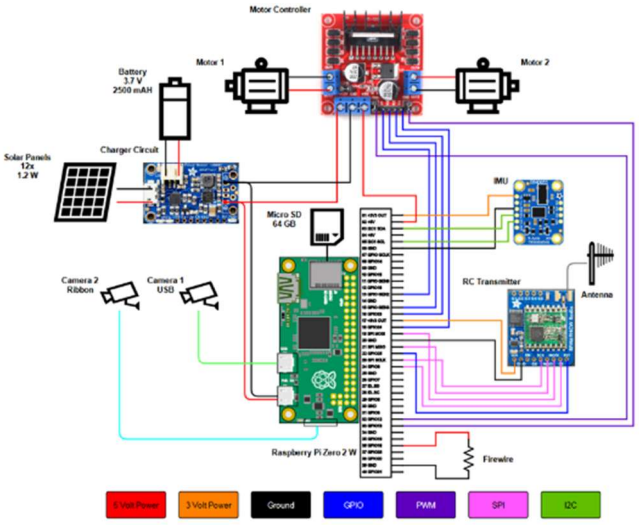

Fig 8: Complete wiring diagram for CubeSat electronics.

D. Computing and Communication

The ability to integrate and process information while providing instructions to subsystems is critical for CubeSat's operation. For this specific mission, a central computer must issue commands to take a picture every minute, analyze and store measured and internal data, and issue commands to send the information to a ground station. Through review of various commercially off-the-shelf systems, a Raspberry Pi was chosen because it can run multiple tasks simultaneously, it enables I/O interfaces, and is universally easy to integrate, along with numerous operation documentation. The dimensions for a Pi Zero 2W made it ideal for the 1.5 U CubeSat form-factor, as well as its power consumption range being comparatively low, between 0.5 – 1.4 W.

The CubeSat required radio communication for transmission of photos, status, and commands. Due to time and budgetary constraints of the project, obtaining a license and equipment for operating space-grade radio communications was not feasible. A radio band not requiring licensing for common use was the 915 MHz band which has a great information bandwidth. Adafruit RFM95W was selected as the transceiver for this band because of its omnidirectional operation, making the location of the radio within the CubeSat a secondary consideration in design. A LoRa (Long Range) radio was used to make up for the range lost by selecting the higher frequency. The radio is a packet radio with automatic error correction.

The radio can transmit at 19.2 Kbps, meaning over a 45-minute period it can send 6154 KB of information, including a 5% margin of error transmission. Transmitting images will consume the most bandwidth, therefore, to send 90 images taken throughout the revolution during a 45-minute connection window, each image needs to be compressed to 68.3 KB. Since this is a proof-of-concept design, the radio will only have a range of 500 meters within line of sight. A ground station to receive CubeSat data will be composed using an Adafruit Feather 32u4 RFM95 LoRa radio connected via USB to a laptop. This ground station is controlled using a serial window on the laptop, accessed through the Arduino IDE.

E. Cameras and Control

The main requirement of the CubeSat was to take a picture every minute. Therefore, 2 cameras were selected for redundancy purposes: a RasPi Cam 3 because of its easy integration and coding with the on-board computer, and the M5 Stack ESP Timer 32X camera with its internal battery, integrated timer, and storage for image capture. Both cameras can take pictures in the minimum required resolution, making it easier to process the images. They both follow common connections with the Pi Zero 2W, with the PiCam using a ribbon cable and the M5 Stack connecting through I2C. One of the cameras is not Pi-native hardware, and thus requires the implementation of OpenCV in controlling the webcam for taking pictures and compressing the images.

Furthermore, an active system is needed for the CubeSat's attitude determination and control to accomplish its mission of taking images of the earth. Using reaction wheels proved to be ideal as they do not require fuel and are

simpler than moment gyros. Two wheels were set up with a brushless motor used for driving them. One was placed about the vertical (yaw) axis, with the other responsible for rotating the CubeSat up and down. A 9 DOF IMU guides the flywheels on when and where to spin by collecting data from an accelerometer, magnetometer, and gyroscope. It communicates with the computer via the I2C protocol, powered by a 3.3 V rail for simplicity.

To spin the flywheels, simple 5 V DC motors capable of 2500 RPM were implemented with a stall torque of 21 g*cm. An L298N Motor Driver Board is used to control the motors as it can drive two brushed motors simultaneously. It enables clockwise or counterclockwise rotation and allows independent speed control for the motors using Pulse width modulation signals from the onboard computer. Quantification of the rotational velocity of the flywheels is done in Eq. (3).

$$\omega_{sat} = -\frac{I_{flywheel}}{I_{sat}}\omega_{flywheel} \tag{3}$$

The moment of inertia of the solid cylindrical flywheels at a mass of 80 grams is 1.764 x 10^{-5} kg*m^2. The CubeSat moment of inertia in the deployed solar array configuration was found through CAD to be 0.014 kg*m^2 abouts its vertical axis and 0.01 kg*m^2 about the horizontal axis through its wider side. Given the above moments of inertia and the max motor RPM of 2500 RPM, the attitude control mechanism will be able to rotate the CubeSat at approximately 3.15 RPM about its vertical axis and 4.41 RPM about the other axis. This control system comes with the drawback of the ability to become saturated, which occurs when the CubeSat rotates faster than the controls can account for. A passive recovery system could be implemented to help with rotations greater than a 3.5 RPM tumble, such as having the greatest surface area perpendicular to the orbital direction to incur drag and reduce tumble RPM.

F. Budgeting

The original financial budget for the project of $1,250 was provided, however after additional fundraising, the total budget of the project was $4,321. This covered material costs for manufacturing, totaling $2,216.15, keeping the project under budget.

Additionally, the weight budget was another primary consideration during the design phase. Given 1.5 kg to make the CubeSat, the total structure was theoretically calculated to be 1.342 kg meeting the weight constraints, as shown in Fig 9a. For an even weight distribution, placement of internal components resulted in a CG at location x=2.42 mm, y= -1.29 mm, z = 11.94 mm from the centroid of the CubeSat, corresponded to I_{xx} = 0.004 kg*m^2, I_{yy} = 0.004 kg*m^2, and I_{zz} = 0.002 kg*m^2 in its undeployed state.

a)

Design Group	Components	Group total weight (g)
Structure	Framing, Walls	240
Power	Battery, Panels, Hinges, Control Board	533.6
Payload	Computer, Communications, Camera	60.4
Control	Motor Control Board, Motors, Flywheels	428
Miscellaneous	Wires, Epoxy, etc.	80
Total Weight (g)		**1342**

b)

Component	Max. Power req. (W)	Idle Power (W)	Operational Percentage
Raspberry Pi Zero 2W	1.4*	0.5	100
Camera 1	0.75	0.1	5
Camera 2	1	0.5	0**
Communication	0.33	0.005	11
IMU	0.009***	0.0001	100
Attitude Control	0.4	0.12	50
Miscellaneous Draws	0.5	NA	100

*Assumed to be operating at 50% between power consumption modes
**Camera 2 is a backup; functions on camera 1's failure.
***The IMU has a low power mode; switches between standby (80%) and operation (20%)

Fig 9: Weight (a) and Power (b) budgets.

Lastly, each component's power draw was understood to analyze the power budget. As not all components will require max power during orbit, certain component's power draw can be reduced. Fig 9b shows components and their operational time during orbit as a percentage. By multiplying the max power requirement by its operational percentage, multiplying idle power and operational percentage, and summing these values for all components, an average power requirement for the CubeSat is found to be 2.34 W. This is well below the available 7.2 W and will not fully drain the battery containing 3.3 Wh of power during the 45-minute blackout period. The instantaneous max power requirement is found to be 4.4 W, which is below the available from both the solar panels and the battery, satisfying power budget.

V. Manufacturing

The CubeSat manufacturing had minimal deviations from the design phase, due to both design accuracies, as well as overall time constraints on the project, with exceptions to aspects of solar array and camera equipment. Four 10 mm x 10 mm t-slot aluminum extrusions were used with 1 mm thick aluminum sheets to manufacture the internal structure. This material and bending process was sourced from a laser cutting company, SendCutSend. These thin

walls and frames were attached using M3x4 bolts for both the internal and external wall structure. Spring hinges were adhered to the solar panels and then bonded to the CubeSat structure. The intermediary assembly of the CubeSat internal structure with the LiPo for scale, as well as the completed product can be seen in Fig 10. Measuring the CubeSats weight, the total structural mass was 432 g, nonstructural mass was 861 g, for a total mass of 1293 g.

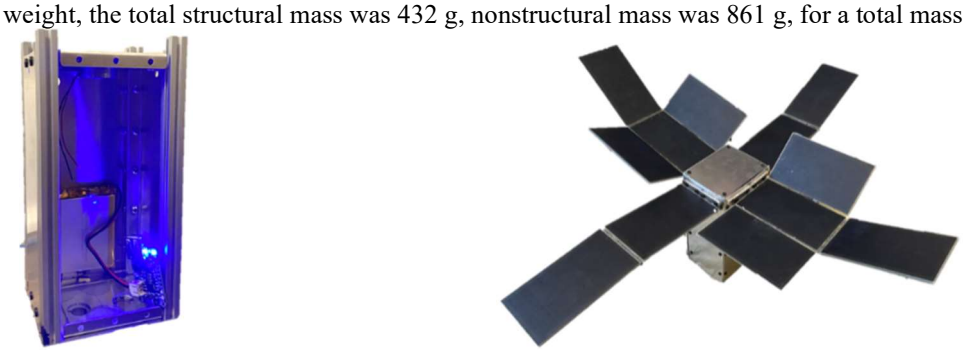

a) b)

Fig 10: Intermediary CubeSat structure (a) and Completed assembly structure (b).

The solar array assembly was altered from using only epoxies to a combination of mechanical fixtures and epoxies due to bonding issues. Attempts with prolonged epoxy application and high pressure failed to secure the structure. Glue layers supported the solar panels on hinges, fixed to c-channels along CubeSat walls through bolts. Due to time constraints, aluminum c-channels bonded to the structure with adhesives, though not ideal for space use, served the proof-of-concept purpose. Glues and epoxies detached from components within hours to days, indicating an impractical long-term solution. Ideally, a mechanical harness around the solar panels would have been preferred, however manufacturing delays and project time constraints made it unfeasible.

For power generation, the 12 solar panels were connected in parallel using 20 AWG wires to the power management circuit. A 2500 mAh LiPo battery was connected to the power management circuit providing power to the Raspberry Pi, in turn acting as a power distributor for all devices. The entire wire bundle for the internal CubeSat components is seen in Fig 11.

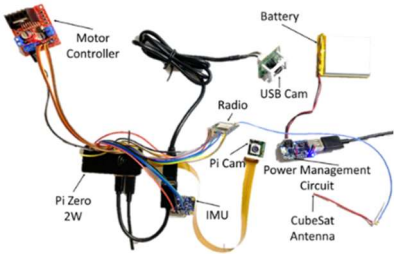

Fig 11: External Testing Wire Configuration.

The flywheels for the active control system were connected to the 3V DC 2400 RPM motors and were made using low carbon steel. Control commands are based on orientation inputs received from the IMU interacting with the Pi. The flywheel diameter was machined to 43 mm with thickness of 7 mm, with center holes drilled to provide a mounting point for a connection to the motor.

A design change was made to replace the M5 Stack camera with a smaller camera with equivalent power consumption due to its form factor. The CubeSat was programmed to capture and save up to 50 photos so that the Pi would only need to store 45 photos during revolution segments before transferring all the photos to the ground station at once. The communication system uses the Feather 32u4 RFM95 LoRa Radio on the ground station and RFM95W radio and is designed to constantly listen for commands while connected to the Pi while changing the output to send information to the ground station. The ground station is coded in C++, and the information transfer between the radio and station is completed using byte arrays, which is where the images are encoded in base 64 and then split into packets due to data transfer limits. Other simpler data structures were directly converted to byte arrays for transfer. Information is received by the station and displayed in the Arduino IDE, later converted to Python for verification.

VI. Testing

The CubeSat's success is determined by individual components, so each of them need to be tested in stages to determine their success of integration. This includes data storage and transfer, power, array deployment, and attitude

determination and control. Fig 12 demonstrates the data storage and transfer capabilities. The left of the image shows how the data is stored, with the right part showing the image location and naming convention.

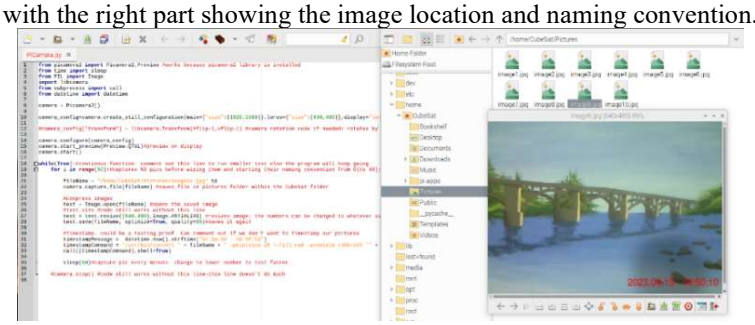

Fig 12: Details of storing an image.

A sample image stored on the Pi was then transferred to the ground station, with a successful result of the hex color code decrypting into pixels of the transmitted image in Fig 13. Most test images were perfectly transmitted; however, some were distorted, possibly due to errors in transmission that time did not allow for fixing.

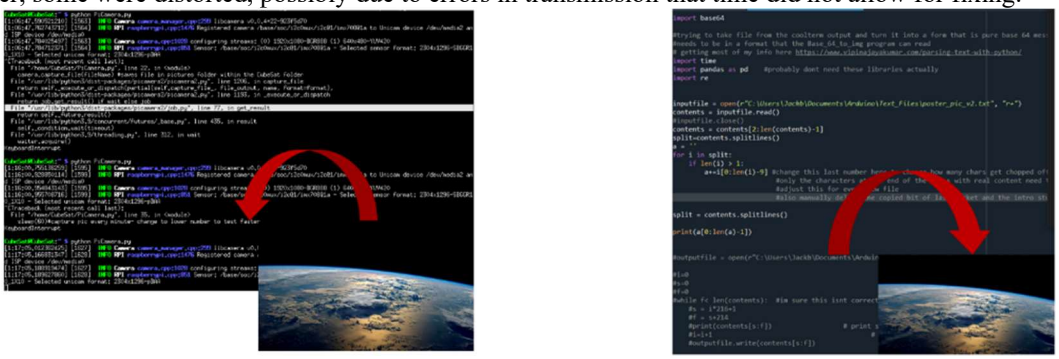

a) b)

Fig 13: Image sent from Pi (a) and Received at ground station (b).

The power management system was tested by cycling the CubeSat under outdoor light in 45-minute cycles of light and dark. The battery was initially at 2/3rd charge and was charged in the sunlight before light was obscured for 90 minutes to obtain accurate discharge characteristics of the system. The CubeSat was then exposed to light for full recharging, with the measurements taken every two minutes. The graph of this battery cycle is seen in Fig 14 with the batteries max voltage being 4.2 V and its minimum being 3.5 V.

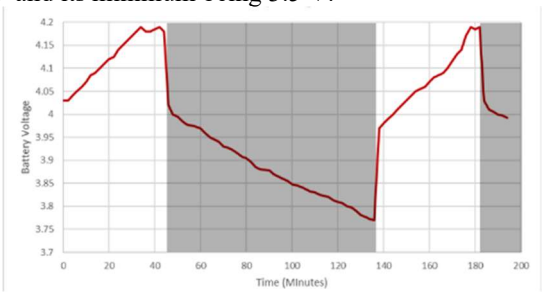

Fig 14: Battery voltage during charge and discharge states.

The array deployment was done using 2 tests. First, the hinges were assessed to see if they could unfold the weight of the combined solar panels. The hinges operated as expected, and had their springs intentionally weakened to not shock load the panels on opening. Deployment in microgravity was simulated by orienting the CubeSat on each side and observing what the hinges would do without a downward moment on the panels, resulting in both the 2 panel and 4 panel configurations successfully deployed. The release mechanism for the deployment of solar panels included the installment of nichrome wire connected to the internal system to rapidly heat up and cut through the panels' binding.[5] This worked as intended with 5 successful tests.

To test attitude determination and control, the CubeSat was suspended by a wire from 2 different orientations about its flywheels. This allowed the wire tension to counteract the gravity experienced by the CubeSat while not providing

torsional resistance. The rotation command was issued from the ground station to the Pi, which was sent to the IMU where the orientation data was queried. The CubeSat was found capable of rotating about its vertical axis at a rate of 8.57 RPM. The initial miscalculations in the code due to the offset of the IMU from the CG in the CubeSat were later corrected after initial testing.

VII. Conclusion

A. Standards Evaluation and Impact

Standards are crucial for CubeSat functionality in both Earth and space environments. While ever evolving, CubeSat standards are fewer compared to aircraft due to the novelty of space exploration. Notably, NASA sets standards like GSFC-STD-7000B for environmental verification which encompasses many standards from criteria listing unsatisfactory performance, to verification requirements of all systems. ISO 17770:2017 standardizes CubeSat sizing, deployment, and assurance. The CubeSat adheres to 1.5U dimensions, while appropriately meeting mass requirements. However, as this standard also mandates deployer verification, the deployer design lacked details due to constraints on the mission success being considered on the Earth, requiring future iterations, which will consider a launch, to comply. Future compliance for deployer design entails acquiring mockups for space simulation and testing. Radio frequency selection, vital for Earth communication, adheres to FCC regulations like Title 47 CFR 15.247, with the chosen 915 MHz frequency offering superior bandwidth and compliance with digital modulation standards.

Additionally, CubeSat's reliance on solar energy not only reduces environmental impact but also eliminates the disposal issue of the alternative of single-use batteries. Its custom-made structure, efficient for this functionality, can be repurposed for other ventures or recycled due to its aluminum composition. Furthermore, the CubeSat's modular design facilitates component breakdown and reusability, minimizing waste and extending each part's lifespan. Even complex elements like solar panels can be repurposed, contributing to environmental sustainability. Regarding potential space deployment, the CubeSat's small size ensures it burns up upon reentry, averting space debris concerns. For a potential launch, considerations about satellite imaging regulations and international policies would be vital.

Moreover, with being unique in the field of exploration and functionality of a CubeSat at the University of South Carolina, this project serves a key role in igniting interest in space exploration among students. Its potential to attract more aerospace projects to South Carolina can foster economic and educational growth, opening doors for partnerships and job opportunities. Lastly, the CubeSat's modular nature enables remote research in space, offering a safe and cost-effective alternative to crewed missions. Mass production and experimentation could yield valuable insights for deep space exploration, benefiting society at large.

B. Further Work

The current CubeSat design is successful in meeting project requirements, but with additional time, significant enhancements are possible. Improvements in code functionality, particularly in communication control, could enable handling various requests such as adjusting picture parameters and packet sizes for more efficient data transfer. Additionally, enhancements to solar panel control, including a sun tracker and rotating hinges, would provide greater flexibility in CubeSat maneuvering. Implementing features like solar panel folding would streamline testing processes and save time. For potential orbit deployment, selecting radiation-hardened components could enhance protection against ionizing particle strikes. Potential launch for diverse use cases leaves room for design improvement.

Acknowledgments

This work was supported in part by the South Carolina Honors College Senior Thesis/Project Grant D.S., S.J., J.H., & P.B. This work was supported in part by funding from the University of South Carolina Mechanical Engineering Department. The team would like to thank Dr. Wout De Backer for his advisement and support throughout the duration of the project.

References

[1]Gujar, Suraj. "Small Satellite Market Size & Share: Global Report, 2032." *Global Market Insights Inc.*, May 2023.

[2]Thyrso Villela, Cesar A. Costa, Alessandra M. Brandão, Fernando T. Bueno, Rodrigo Leonardi, "Towards the Thousandth CubeSat: A Statistical Overview", *International Journal of Aerospace Engineering*, vol. 2019, 13 pages, 2019.

[3]Larson, W. J., & Wertz, J. R. (2005). *Space mission analysis and design* (3rd ed.). Kluwer Academic Publishers.

[4]Low, Y. W., & Chia, Y. X. "Assessment of Orbital Maintenance Strategies for Small Satellites," 32nd AIAA/USU Conference on Small Satellites.

[5]NASA, "CubeSat 101: Basic Concepts and Processes for First-Time CubeSat Developers," October, 2017.